

Aromatic versus Benzylic CH Bond Activation of Alkylaromatics by a Transient η^2 -Cyclopropene Complex

Cédric Boulho,^{†,‡} Laure Vendier,^{†,‡} Michel Etienne,^{*,†,‡} Abel Locati,[§] Feliu Maseras,^{§,⊥} and John E. McGrady[#]

[†]LCC (Laboratoire de Chimie de Coordination), CNRS, 205 Route de Narbonne, F-31077 Toulouse, France

[‡]UPS, INPT, LCC, Université de Toulouse, F-31077 Toulouse, France

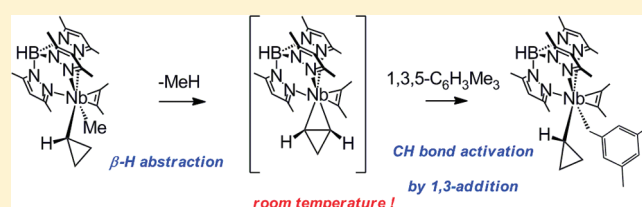
[§]Institute of Chemical Research of Catalonia (ICIQ), Avinguda Països Catalans 16, 43007, Tarragona, Spain

[⊥]Unitat de Química Física, Edifici Cn, Universitat Autònoma de Barcelona, 08193 Bellaterra, Catalonia, Spain

[#]Department of Chemistry, Inorganic Chemistry Laboratory, University of Oxford, South Parks Road, Oxford, OX1 3QR, United Kingdom

S Supporting Information

ABSTRACT: The methyl cyclopropyl hydrotris(3,5-dimethylpyrazolyl)borate complex $\text{Tp}^{\text{Me}_2}\text{NbMe}(c\text{-C}_3\text{H}_5)(\text{MeCCMe})$ reacts smoothly with different alkylaromatics XH at 308 K to yield methane and $\text{Tp}^{\text{Me}_2}\text{NbX}(c\text{-C}_3\text{H}_5)(\text{MeCCMe})$. NMR data show that for mesitylene and 1,4-dimethylbenzene, selective benzylic CH bond activation is observed, giving the benzyl cyclopropyl complexes $\text{Tp}^{\text{Me}_2}\text{Nb}(\text{CH}_2\text{Ar}')(c\text{-C}_3\text{H}_5)(\text{MeCCMe})$ ($\text{Ar}' = 3,5\text{-Me}_2\text{C}_6\text{H}_3, 4\text{-MeC}_6\text{H}_4$, respectively). Selective arene CH bond activation is observed with 1,2-dimethylbenzene, yielding $\text{Tp}^{\text{Me}_2}\text{Nb}(3,4\text{-Me}_2\text{C}_6\text{H}_3)(c\text{-C}_3\text{H}_5)(\text{MeCCMe})$. With 1,3-dimethylbenzene, a 3:1 mixture of arene and benzylic CH activated products, $\text{Tp}^{\text{Me}_2}\text{Nb}(3,5\text{-Me}_2\text{C}_6\text{H}_3)(c\text{-C}_3\text{H}_5)(\text{MeCCMe})$ and $\text{Tp}^{\text{Me}_2}\text{Nb}(\text{CH}_2\text{-}3\text{-MeC}_6\text{H}_4)(c\text{-C}_3\text{H}_5)(\text{MeCCMe})$, is observed, translating to a 18:1 preference for aromatic versus benzylic CH bond activation on a per CH bond basis. Kinetic studies are consistent with rate-limiting intramolecular β -H abstraction of methane to yield a transient unsaturated η^2 -cyclopropene intermediate. This intermediate reacts rapidly with the aromatic or benzylic CH bond of the arene via 1,3-addition across a Nb(η^2 -cyclopropene) bond. DFT calculations suggest that the observed selectivities are a result of the steric influence of the methyl groups on the arene ring, which blocks activation of an *ortho* C–H bond.



INTRODUCTION

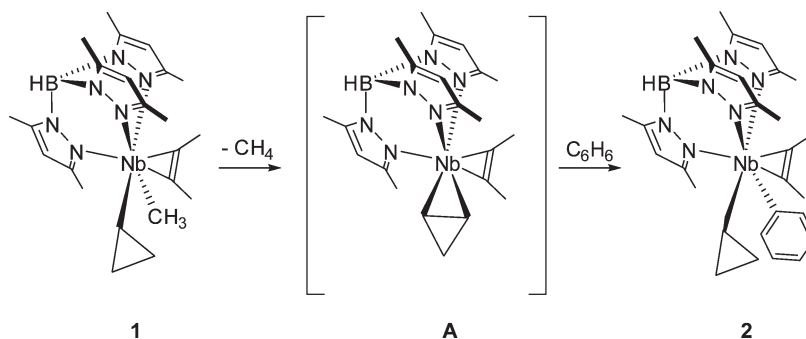
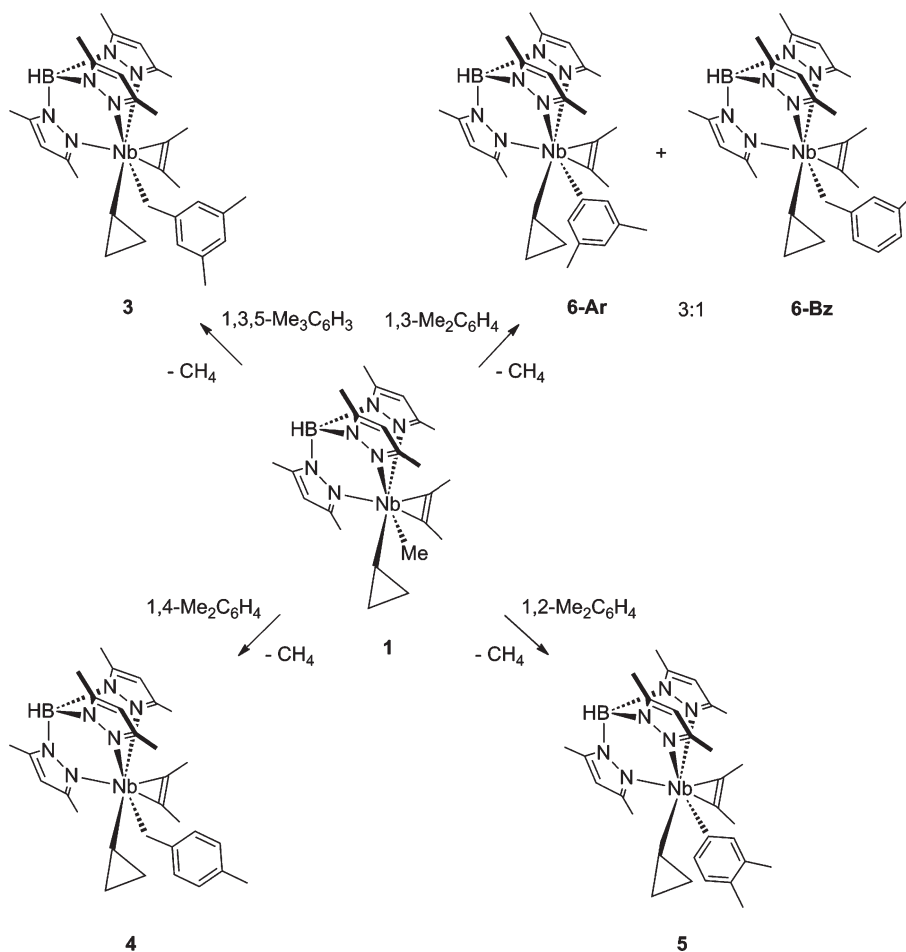
Even though CH bond activation reactions have become a practical tool for synthetic chemists in recent years,¹ the search for new reactions and a deeper understanding of the underlying mechanisms remains an active area of research.² We recently reported (Scheme 1) that the α -CC agostic methyl cyclopropyl complex $\text{Tp}^{\text{Me}_2}\text{NbMe}(c\text{-C}_3\text{H}_5)(\text{MeCCMe})$ (**1**) undergoes intramolecular elimination of methane at room temperature to yield an unsaturated η^2 -cyclopropene intermediate, $[\text{Tp}^{\text{Me}_2}\text{Nb}(\eta^2\text{-}c\text{-C}_3\text{H}_4)(\text{MeCCMe})]$ (**A**). This then reacts with benzene to give the phenyl cyclopropyl complex $\text{Tp}^{\text{Me}_2}\text{NbPh}(c\text{-C}_3\text{H}_5)(\text{MeCCMe})$ (**2**) via a 1,3-addition of the CH bond across a Nb–C bond of the Nb(η^2 - $c\text{-C}_3\text{H}_4$) moiety.³

There are a number of well-established pathways that lead to intermolecular activation of unactivated hydrocarbon CH bonds by complexes of early transition metal ions. For example, σ -bond metathesis at d^0 complexes, where no formal coordination of the hydrocarbon occurs prior to formation of a kite-shaped four-center transition state, has been established by seminal work on scandium derivatives.⁴ The formation of intermediates with unsaturated M=C bonds, such as those generated by α -H

abstraction reactions in dialkyl complexes of groups 4–6, offers an alternative route. These complexes are capable of activating hydrocarbon CH bonds by a 1,2-addition across the M=C bond.⁵ This reaction type was recently extended to transient titanium alkylidene intermediates (a 1,2-addition of the CH bond across a Ti=C bond).⁶ β -H abstraction pathways such as that illustrated in Scheme 1 are, in contrast, extremely rare.⁷ The best characterized examples occur in alkyl phenyl or diphenyl complexes $\text{L}_n\text{MR}(\text{Ph})$, where β -H abstraction of a hydrocarbon RH from an *ortho* hydrogen yields benzyne complexes. These unsaturated benzyne intermediates are also capable of the reverse reaction, a 1,3-addition of a hydrocarbon CH bond across a M–benzyne bond.⁸ η^3 -Allyl alkyl and vinyl alkyl complexes of molybdenum and tungsten also generate unsaturated η^2 -allene, η^2 -diene, and η^2 -alkyne complexes, respectively, by β -H abstraction, and these intermediates are also able to cleave CH bonds of various hydrocarbons.⁹ However, simple unsaturated η^2 -alkene intermediates such as **A** have clearly been underestimated as

Received: March 4, 2011

Published: July 06, 2011

Scheme 1. CH Bond Activation of Benzene by a Transient η^2 -Cyclopropene SpeciesScheme 2. Reactions of $\text{Tp}^{\text{Me}_2}\text{NbMe}(c\text{-C}_3\text{H}_5)(\text{MeCCMe})$ (**1**) with Alkylaromatics

competent CH bond activating species. Given the novelty and the very mild conditions of the reaction summarized in Scheme 1, we decided to study its scope in more detail. In this paper we report a joint experimental and computational study of the selectivity of intermediate **A** for $\text{Csp}^3\text{-H}$ versus $\text{Csp}^2\text{-H}$ bond activation in alkyl aromatics. Our results offer an interesting comparison to related studies for 1,2-CH bond activations at $\text{M}=\text{C}$, $\text{M}=\text{NR}'$, and $\text{Ti}\equiv\text{C}$ bonds and to oxidative addition reactions.

RESULTS AND DISCUSSION

Reactions of Alkyl Aromatics. The reactivity of the methyl cyclopropyl complex $\text{Tp}^{\text{Me}_2}\text{NbMe}(c\text{-C}_3\text{H}_5)(\text{MeCCMe})$ (**1**) with various alkylaromatics is summarized in Scheme 2. **1** reacts smoothly at 308 K with mesitylene (either pure or in cyclohexane solution) over the course of 12 h to give the substituted benzyl cyclopropyl derivative $\text{Tp}^{\text{Me}_2}\text{Nb}(\text{CH}_2\text{-}3,5\text{-Me}_2\text{C}_6\text{H}_3)(c\text{-C}_3\text{H}_5)(\text{MeCCMe})$ (**3**). Monitoring the reaction in cyclohexane- d_{12} in

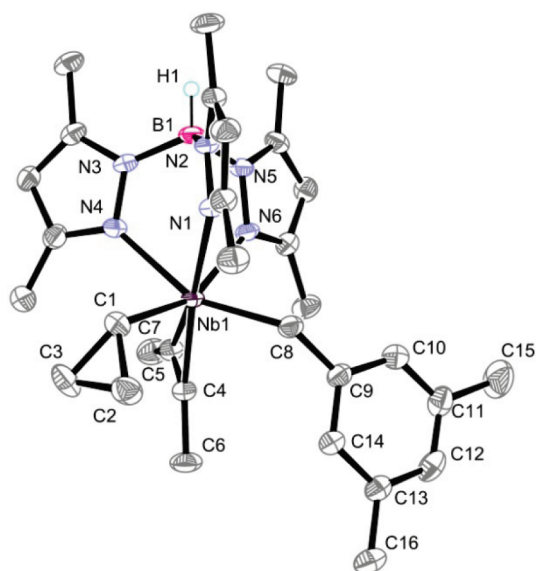


Figure 1. Plot of the X-ray molecular structure of $\text{Tp}^{\text{Me}_2}\text{Nb}(\text{CH}_2\text{-}3,5\text{-Me}_2\text{C}_6\text{H}_3)(c\text{-C}_3\text{H}_5)(\text{MeCCMe})$ (**3**).

Teflon-valve sealed NMR tubes reveals that, along with some unidentified decomposition products, complex **3** is formed selectively. No signals attributable to any aryl complex (i.e., a broad yet prominent niobium-bound aryl carbon in the δ 190 region; see below) were observed. This establishes that selective benzylic CH bond activation occurs in mesitylene. Key ^1H NMR data include an AB-type pattern for the diastereotopic benzylic protons of NbCH_2 at δ 2.93 and 2.85 (both d, $^2J_{\text{HH}} = 11.5$ Hz) and two singlets at δ 6.52 and 6.45 in a 2:1 ratio, assigned to *ortho* and *para* protons on the aryl ring. The appearance of a single aromatic ring methyl resonance at δ 2.20 integrating for six protons confirms free rotation about the CH_2 –arene bond. In the ^{13}C NMR spectrum, the benzylic carbon appears as a triplet at δ 77.2 with a $^1J_{\text{CH}}$ of 117 Hz establishing η^1 -benzyl coordination. Protons of the cyclopropyl group give ^1H NMR multiplets in the δ 1.94–0.93 region, and the niobium-bound carbon appears as a prominent doublet at δ 65.3 ($^1J_{\text{CH}} = 138$ Hz).

Both the nature of complex **3** and the coordination mode of the benzylic ligand were confirmed by an X-ray diffraction analysis (Figure 1). An obtuse Nb–C α –Cipso angle of $134.3(2)^\circ$ and large Nb \cdots Cipso (3.4 Å) and Nb \cdots Cortho (4.1, 4.4 Å) distances testify to an η^1 -bound 3,5-dimethylbenzyl ligand. The obtuse Nb–C α –Cipso angle and the conformation of the benzylic ligand, which directs the 3,5-dimethylaryl ring away from the Tp^{Me_2} ligand (Nb(1)–C(8)–C(9)–C(10) 106°), are most likely due to steric reasons. The Nb–C α bond length of 2.220(3) Å for the benzyl ligand is notably greater than the value of 2.188(3) Å for the Nb–C α of the cyclopropyl ligand. As observed in related cyclopropyl complexes,^{3,10} the cyclopropyl ligand adopts a characteristic conformation with the C α –C β bond oriented roughly in the C α –Nb–C α' plane (C(2)–C(1)–Nb–C(8) -37°). The C(1)–C(2) distance (1.539(5) Å) is slightly longer than C(1)–C(3) (1.518(5) Å), although the difference is barely significant here. With the distortion revealed by different Nb–C α –C β angles [Nb–C(1)–C(2), $118.6(2)^\circ$; Nb–C(1)–C(3), $130.2(3)^\circ$], these data are indicative of a possible α -CC agostic structure.¹¹

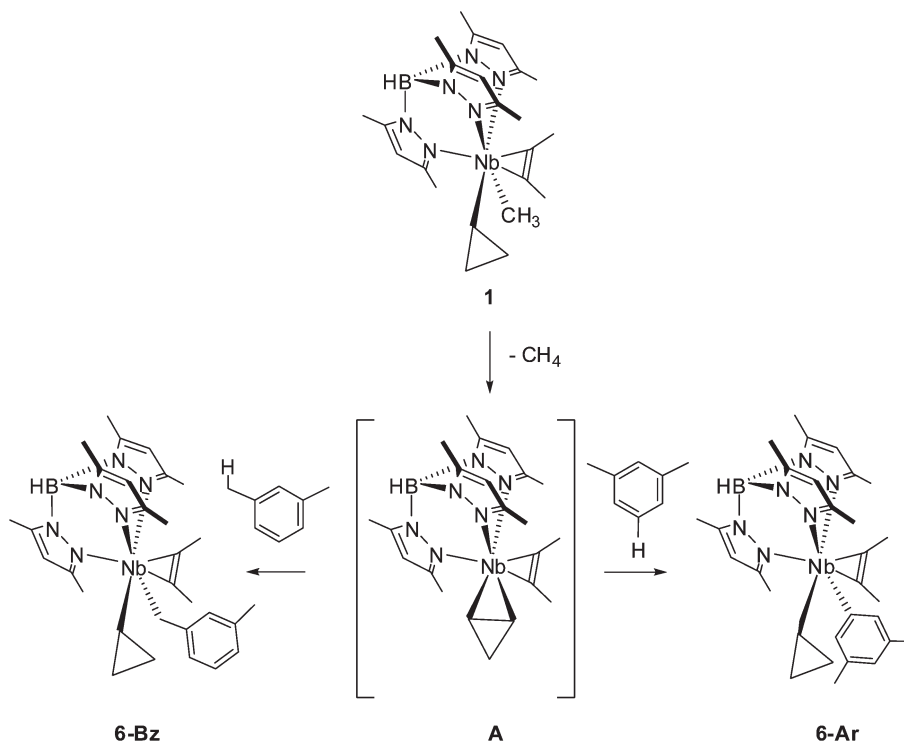
We now turn to the reaction of **1** with dimethylbenzenes, as depicted in Scheme 1. Reaction of **1** with 1,4-dimethylbenzene under similar conditions to those described for mesitylene again selectively yields a benzylic-type product, $\text{Tp}^{\text{Me}_2}\text{Nb}(\text{CH}_2\text{-}4\text{-C}_6\text{H}_4\text{Me})(c\text{-C}_3\text{H}_5)(\text{MeCCMe})$ (**4**), with similar key spectroscopic data to those for **3** (see Experimental Section). Both benzylic complexes **3** and **4** readily react with benzene to yield the phenyl cyclopropyl complex **2**.³ At room temperature, and again despite some decomposition, a single product, **5**, results from the reaction of **1** with one equivalent of 1,2-dimethylbenzene.¹² Note that under similar conditions **1** decomposes even more extensively in the absence of arene. Characteristic ^1H and ^{13}C NMR signals of benzylic products are conspicuously absent, and **5** can be identified as the aryl cyclopropyl complex $\text{Tp}^{\text{Me}_2}\text{Nb}(c\text{-C}_3\text{H}_5)(3,4\text{-Me}_2\text{C}_6\text{H}_3)(\text{MeCCMe})$. In the ^1H NMR spectrum of **5**, two aromatic signals at δ 7.04 and 6.81 integrating for 2H and 1H, respectively, are observed at room temperature, indicating a fluxional process. A characteristic ^{13}C NMR signal at δ 190.9 points to the presence of an aromatic ring bound to niobium. Decoalescence of the ^1H NMR signals is observed upon cooling at 193 K in dichloromethane- d_2 . The characteristic pattern of one singlet (δ 8.16) and two doublets (δ 6.44 and 5.71, $^3J = 14$ Hz) integrating to one H each gives evidence that methyl groups are in positions 3 and 4 of the aryl ring in **5**, as shown in Scheme 1.

In marked contrast to either 1,2- or 1,4-dimethylbenzene, CH bond activation in 1,3-dimethylbenzene is not selective (Scheme 1). The reaction between **1** and 1,3-dimethylbenzene yields an inseparable 3:1 mixture of aryl $\text{Tp}^{\text{Me}_2}\text{Nb}(3,5\text{-Me}_2\text{C}_6\text{H}_3)(c\text{-C}_3\text{H}_5)(\text{MeCCMe})$ (**6-Ar**) and benzylic $\text{Tp}^{\text{Me}_2}\text{Nb}(\text{CH}_2\text{-}3\text{-MeC}_6\text{H}_4)(c\text{-C}_3\text{H}_5)(\text{MeCCMe})$ (**6-Bz**) complexes resulting from aromatic or benzylic CH bond activation, respectively, along with unidentified decomposition products as above. Despite these drawbacks, ^1H and ^{13}C NMR data can be analyzed. In the ^{13}C NMR spectrum, a single aryl carbon resonance at δ 193 and a benzylic resonance at δ 77.1 are assigned to **6-Ar** and **6-Bz**, respectively. The niobium-bound carbon of the $c\text{-C}_3\text{H}_5$ rings is observed at δ 70.5 and 66.3, respectively. This 3:1 ratio translates to an 18:1 preference for aromatic activation of the 5-CH bond over benzylic CH activation on a per CH bond basis.

Overall these experiments indicate that aromatic CH bond activation is preferred over benzylic CH bond activation in alkylbenzenes, the latter only becoming competitive when steric congestion is present. Selective benzylic CH activation is observed for 1,4-dimethylbenzene and mesitylene but not for 1,2-dimethylbenzene, establishing that activation of an aromatic CH bond or of a benzylic CH bond *ortho* to at least one methyl group is strongly disfavored. The case of 1,3-dimethylbenzene is particularly significant in this regard since it is the only case where both aromatic and methyl C–H groups that do *not* lie *ortho* to an Me substituent are available. Consequently in this case, competitive benzylic and aromatic activation are observed.

Kinetic Studies. The kinetic behavior of the reaction between **1** and mesitylene has been studied in detail to verify that the mechanism previously established for the reaction between **1** and benzene was still operational. The reaction converting **1** to **3** (^1H NMR, cyclohexane- d_{12} , $T = 308$ K) is first-order in **1** and zeroth-order in mesitylene (established using 1, 2, 8, and 15 equiv of mesitylene versus **1**) with $k_{\text{obs}} = (5.67 \pm 0.07) \times 10^{-5} \text{ s}^{-1}$, a rate constant equal to that of the reaction of **1** with benzene under the same conditions.³ The same value of k_{obs} was observed when **1** was reacted with 1,4-dimethylbenzene, and no kinetic

Scheme 3. Aromatic versus Benzylic CH Bond Activation of 1,3-Dimethylbenzene by Intermediate A



isotope effect or incorporation of deuterium in evolved methane (δ 0.21 in cyclohexane- d_{12}) was seen when 1,4-dimethylbenzene- d_{10} was activated under identical conditions ($k_H/k_D = 1.0 \pm 0.1$ at 308 K). These experiments indicate that whatever the nature of the arene (benzene, mesitylene, or 1,4-dimethylbenzene), the rate-determining step consists of intramolecular elimination of methane from **1** by β -H abstraction to yield an unsaturated η^2 -cyclopropene intermediate **A**. **A** then rapidly activates an aromatic or benzylic CH bond of the arene to give the products.³ The available pathways in the case of the nonselective activation of 1,3-dimethylbenzene are depicted in Scheme 3.

We have also monitored the reaction between **1** and 15 equiv of 1,3-dimethylbenzene by ^1H NMR in cyclohexane- d_{12} at 308 K. The ratio between **6-Ar** and **6-Bz** remains constant throughout the reaction, suggesting that the final product distribution results from kinetic rather than thermodynamic selectivity.³ This view is further substantiated by computational studies (see below) that indicate aryl complexes are preferred by ca. $20 \text{ kJ}\cdot\text{mol}^{-1}$. It could not be established whether interconversion was occurring at longer reaction times or higher temperatures due to extensive decomposition, but again computational studies suggest it would not.

Computational Studies. In this section we report a series of calculations performed with density functional theory (PBE1PBE/LanL2DZ(+f), 6-31G(d)), the aim being to confirm the structure of the key intermediates and transition states identified above and to identify the origin of the energetic differences between them. The optimizations on the mesitylene system allow us to benchmark the calculations since the X-ray molecular structure of **3** is known. We have identified three distinct rotamers of the mesitylene complexes, all of which are presented in Figure 2. The first and most stable one has a conformation very

similar to the X-ray structure, while the second, which connects directly to the important C–H bond activation transition state (*vide infra*) lies $7 \text{ kJ}\cdot\text{mol}^{-1}$ higher. The third rotamer, where the mesityl ligand lies in the wedge defined by two pyrazolyl rings, lies $5 \text{ kJ}\cdot\text{mol}^{-1}$ above the lowest energy structure. Apart from the conformation of the mesityl ring, all three structures have very similar bond lengths and angles.

A representative potential energy surface for the reaction of intermediate **A** with 1,4-dimethylbenzene is shown in Figure 3. The surfaces for the other substrates are qualitatively similar and are shown in the Supporting Information. The energies of the key stationary points are collected in Table 1. Our focus here is on selectivity issues for aromatic versus benzylic CH bond activations by a common intermediate **A**, so we do not discuss the details of the elementary step originating from **1** except to note that intermediate **A** (plus methane) lies $48 \text{ kJ}\cdot\text{mol}^{-1}$ above **1** and the transition state for the β -H abstraction of methane leading to **A** is $116 \text{ kJ}\cdot\text{mol}^{-1}$ above **1**.

Table 1 reveals that the benzylic activation pathway is very similar for all substrates: the four key transition states have relative energies between 69 and $74 \text{ kJ}\cdot\text{mol}^{-1}$. Thus the selectivity arises primarily from variations in the aromatic pathway, which are determined by the number of methyl groups *ortho* to the metalated carbon. Where there are no *ortho* methyls (1,2-dimethylbenzene and 5-H activation in 1,3-dimethylbenzene) the transition states have relative energies of 60 and $61 \text{ kJ}\cdot\text{mol}^{-1}$. The presence of one *ortho* methyl (1,4-dimethylbenzene and 4-H activation in 1,3-dimethylbenzene) increases this to $84 \text{ kJ}\cdot\text{mol}^{-1}$, a value that exceeds the narrow range of benzylic activation. Where two *ortho* methyls (mesitylene) are present the barrier rises to $137 \text{ kJ}\cdot\text{mol}^{-1}$. On this basis, the presence of a single *ortho* methyl group should be sufficient to block aromatic C–H activation and cause a switch to the benzylic pathway. For the

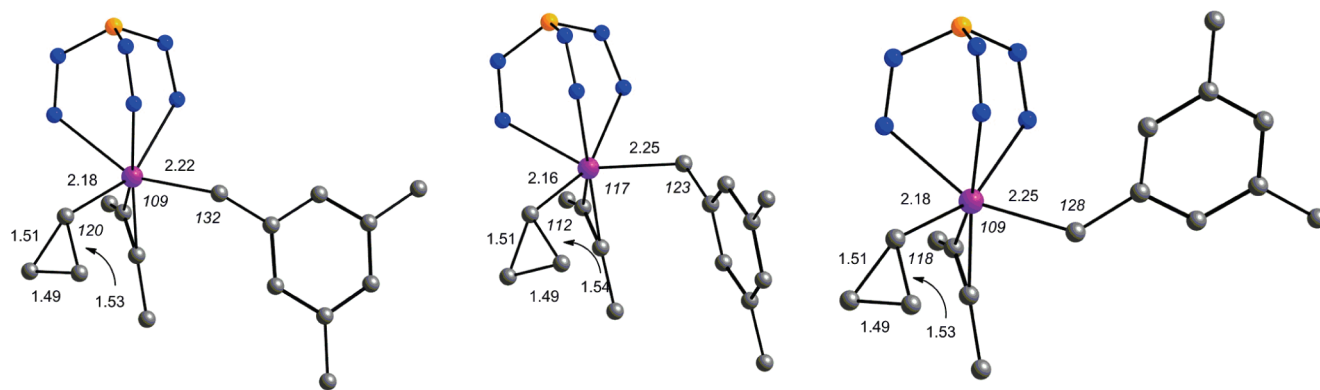


Figure 2. DFT-optimized structures of $\text{Tp}^{\text{Me}_2}\text{Nb}(\text{CH}_2\text{-}3,5\text{-Me}_2\text{C}_6\text{H}_3)(c\text{-C}_3\text{H}_5)(\text{MeCCMe})$ (**3**). Left, rotamer related to the X-ray structure; center, rotamer linked to the TS for benzylic CH bond activation ($+7 \text{ kJ} \cdot \text{mol}^{-1}$); right, rotamer with the mesityl group in the wedge ($+5 \text{ kJ} \cdot \text{mol}^{-1}$). Hydrogens and Tp^{Me_2} backbone omitted for clarity. Bond distances in Å, bond angles (*italicized*) in deg.

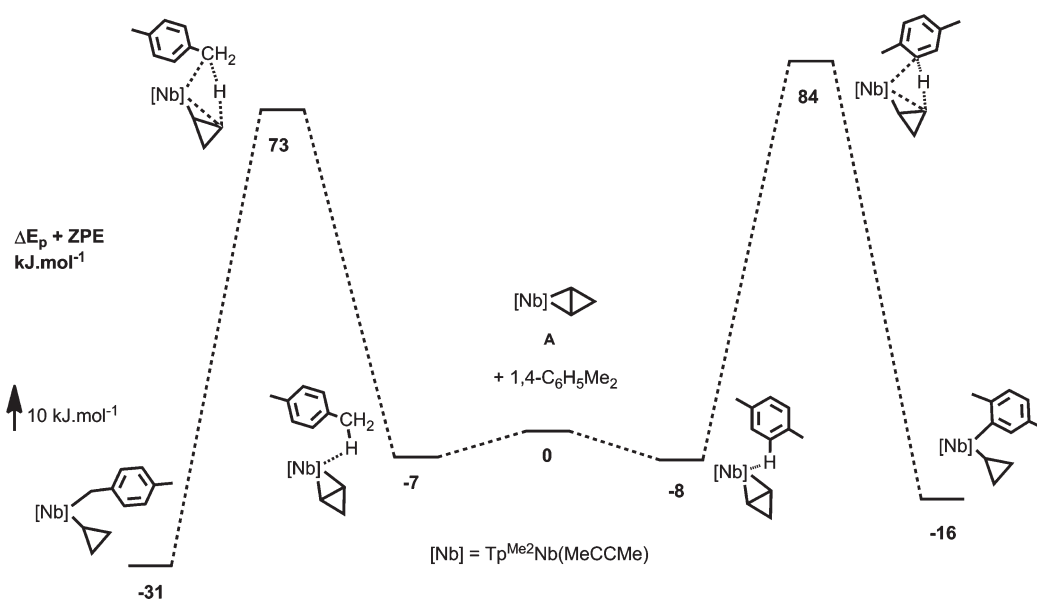


Figure 3. Potential energy (with ZPE corrections) diagram for the benzylic and aromatic CH bonds of 1,4-dimethylbenzene by $[\text{Tp}^{\text{Me}_2}\text{Nb}(\eta^2\text{-C}_3\text{H}_4)(\text{MeCCMe})]$.

Table 1. Computed Potential Energies ($\text{kJ} \cdot \text{mol}^{-1}$) for the Activation of Benzylic and Aromatic CH Bonds of Alkylbenzenes by Intermediate **A**^a

arene	benzyl complex	transition state for benzylic activation	aryl complex		transition state for aromatic activation	
mesitylene	-32	69	45		137	
1,4-dimethylbenzene	-31	73	-16		84	
1,3-dimethylbenzene	-32	73	4-H activation	5-H activation	4-H activation	5-H activation
			-17	-52	84	61
1,2-dimethylbenzene	-25	74	-54		60	

^a Energies include zero-point energy corrections and are relative to **A** + arene.

reaction of **1** with mesitylene, for example, the transition states for benzylic or aromatic activation are 69 or 137 $\text{kJ} \cdot \text{mol}^{-1}$ above **A**, respectively, with a $\Delta\Delta E^\ddagger$ of 68 $\text{kJ} \cdot \text{mol}^{-1}$, and only benzylic activation is observed. The barriers for the two competing processes are closer for 1,4-dimethylbenzene (Figure 3), although

still in favor of benzylic activation (73 vs 84 $\text{kJ} \cdot \text{mol}^{-1}$). The difference of 11 $\text{kJ} \cdot \text{mol}^{-1}$ is small but still compatible with the experimental observation of only benzylic activation.

In the case of 1,3-dimethylbenzene, both benzylic and aromatic activation are experimentally observed. The aromatic

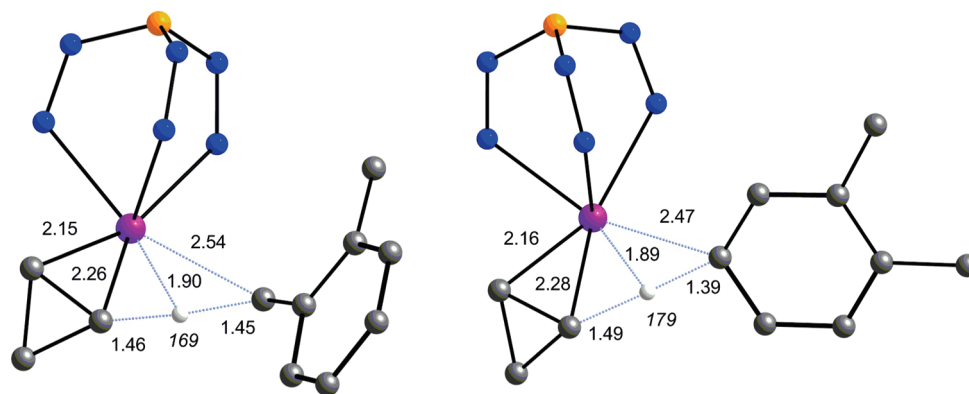


Figure 4. DFT-computed transition states for benzylic and aromatic CH bond activations of 1,2-dimethylbenzene by $\text{Tp}^{\text{Me}_2}\text{Nb}(\eta^2\text{-C}_3\text{H}_4)(\text{MeCCMe})$ (alkyne and Tp^{Me_2} backbone omitted for clarity). Bond distances in Å, bond angles (*italicized*) in deg.

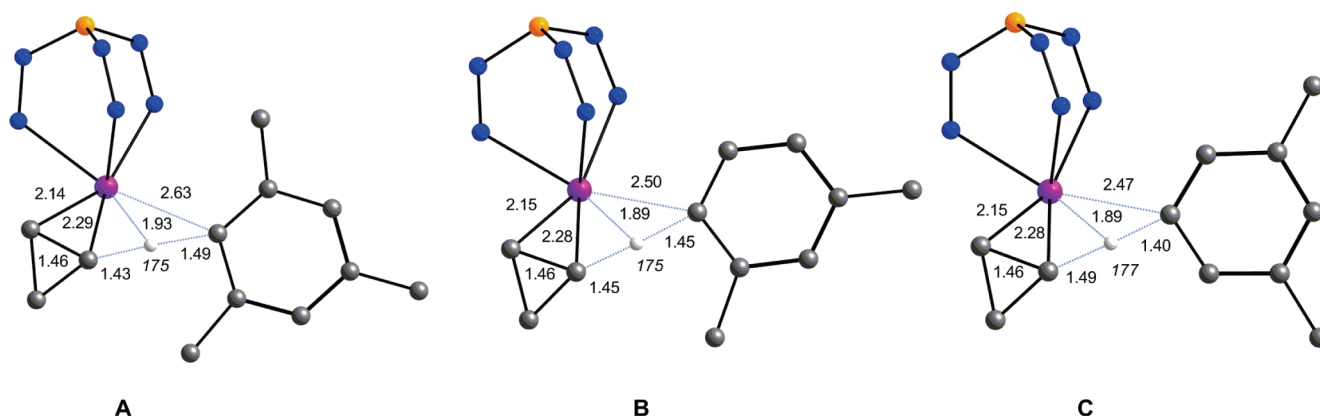


Figure 5. DFT-computed transition states for aromatic CH bond activation of mesitylene (A), 4-CH (B), and 5-CH (C) bonds of 1,3-dimethylbenzene by $\text{Tp}^{\text{Me}_2}\text{Nb}(\eta^2\text{-C}_3\text{H}_4)(\text{MeCCMe})$ (alkyne and Tp^{Me_2} backbone omitted for clarity). Bond distances in Å, bond angles (*italicized*) in deg.

activation is exclusively in the 5-position (no *ortho* CH_3 , barrier of $61 \text{ kJ}\cdot\text{mol}^{-1}$) rather than in the 4-position (and one *ortho* CH_3 , barrier of $84 \text{ kJ}\cdot\text{mol}^{-1}$). The benzylic activation pathway has a barrier of $73 \text{ kJ}\cdot\text{mol}^{-1}$, and the difference in activation energies, ΔE_a , of $12 \text{ kJ}\cdot\text{mol}^{-1}$ should be sufficient to lead to full selectivity. However, we note that benzylic activation is favored statistically over aromatic activation by a ratio of 6:1, and this difference apparently reduces the free energy of activation sufficiently to allow both products to form. We note here that in the cases of mesitylene and 1,4-dimethylbenzene the statistical factor only serves to reinforce the enthalpic preference for benzylic activation.

The computed potential energy profile for 1,2-dimethylbenzene is very similar to that for the 1,3-isomer. However in this case only aromatic activation (at the 4-position) is observed experimentally, a difference that seems inconsistent with the very similar computed barriers to benzylic and aromatic activation ($\Delta E_a = 14 \text{ kJ}\cdot\text{mol}^{-1}$ for 1,2-dimethylbenzene versus $12 \text{ kJ}\cdot\text{mol}^{-1}$ for 1,3-dimethylbenzene). While the statistical factor is 6:1 in favor of benzylic activation for 1,3-dimethylbenzene, the ratio is reduced to 3:1 in the case of 1,2-dimethylbenzene, where two aromatic C–H bonds are available. Thus it appears that statistical factors play a key role in fine-tuning the general reactivity patterns that are determined primarily by the influence of *ortho* methyl groups on the barrier to aromatic C–H activation.

The transition states for CH activation/formation of the benzylic and aromatic CH bond of 1,2-dimethylbenzene are depicted in Figure 4 and have broadly similar structures. There is an almost linear $\text{C}\cdots\text{H}\cdots\text{C}$ geometry for the H transfer between the coordinated and entering hydrocarbons, most notably in the case of the aromatic interaction where the TS is slightly unsymmetrical with a shorter CH bond on the arene side (activation of an aromatic sp^2 CH bond) than on the η^2 -cyclopropene side. At the same time the arene approaches the metal more closely ($\text{Nb}\cdots\text{C}$ 2.47 versus 2.54 Å) in the aromatic activation pathway, leading to a more compressed transition state. The transferred hydrogen carries a similar small positive Mulliken charge in both transition states (0.111 and 0.100; it is the least charged H in both structures), in both cases despite a more negative benzylic (-0.674) versus aromatic (-0.208) carbon. This suggests that the key step can be viewed as a hydrogen atom transfer between the two carbons.

Variations of transition-state geometries for the aromatic CH bond activation with the number of *ortho* methyl groups are pictured in Figure 5. In all cases the alkyne lies roughly parallel to the η^2 -cyclopropene. The Nb–C(Ar) distance is markedly longer (2.63 Å) in the case of mesitylene (two *ortho* methyl groups) than in the cases of 1,3-dimethylbenzene (2.50 Å) (one *ortho* methyl group), 1,3-dimethylbenzene (2.47 Å), and 1,2-dimethylbenzene (2.47 Å) (no *ortho* methyl group), which suggests a steric role for the *ortho* methyl groups. The contraction

of the Nb–C(Ar) distance in the transition state correlates with the energy barrier (A, 137 > B, 84 > C, 61 kJ·mol⁻¹). The transition states appear rather asynchronous, as judged by an inverse trend for the variation of the distances between the two carbons and the hydrogen. For 1,2-dimethylbenzene (Figure 4), the value of 1.39 Å for the C(Ar)–H distance can be compared with values of 1.40 and 1.49 Å for 1,4-dimethylbenzene and mesitylene, respectively. This increase in C(Ar)–H distance is accompanied by a decrease of the C(cyclopropyl)–H distances from 1.49 Å (1,2- and 1,3-dimethylbenzene, activation at C5) to 1.45 Å (1,3-dimethylbenzene, activation at C4) and 1.43 Å for mesitylene.

Having established the key role for *ortho* methyl groups in determining the barrier to aromatic C–H activation, it is important to establish whether this effect has steric or electronic origins. We were able to resolve this question by performing a parallel set of ONIOM(PBE1PBE:UFF) calculations on the aromatic activation in 1,4-dimethylbenzene where one of the methyl substituents is described by a molecular mechanics force field. Within this protocol, the steric demand of the methyl group is retained, but its electronic effect is that of hydrogen. The results of this test are conclusively in favor of a purely steric effect: the computed barrier to aromatic activation is 88 kJ·mol⁻¹, very close to the 84 kJ·mol⁻¹ obtained from a full DFT calculation of this system and far from the ca. 60 kJ·mol⁻¹ characteristic of cases with no *ortho* methyl groups.

The seemingly diverse C–H activation chemistry of these substituted benzenes can therefore be rationalized by a simple set of rules. Overall, there is a small kinetic preference to activate aromatic over aliphatic CH bonds, but only when steric effects are negligible. The presence of *ortho* methyl groups raises the barrier above that for the alternative benzylic activation, causing a switch in mechanism.

Comparisons with Related Systems. In this section we briefly compare our selectivity results with those seen in related systems. Selectivity in C–H bond activation of alkyl aromatics varies across a very broad spectrum. At one extreme, σ -bond metathesis of toluene by Cp*₂ScMe is extremely unselective, yielding products resulting from CH activation at all benzylic and aromatic sites.⁴ Reactions involving unsaturated intermediates related to A have, however, proven to be rather more selective. The groups of Legzdins^{5,9} and Mindiola⁶ have studied competitive CH activation reactions of hydrocarbons by unsaturated molybdenum and tungsten alkylidene complexes and unsaturated titanium alkylidene complexes, respectively, i.e., 1,2-CH bond addition across M=C (M = Mo, W) and Ti=C bonds. Bergman, Horton, and Wolczanski have explored similar reaction chemistry with transient unsaturated d⁰ imido complexes of groups 4 and 5, [L_nM=NR],¹³ while Jones has reported C–H activation chemistry for Cp*₂ and Tp^{Me2}-based complexes of rhodium, in this case via coordinatively unsaturated intermediates such as Tp^{Me2}Rh(CNCMe₃).^{14,15}

With mesitylene as substrate, benzylic C–H activation is the exclusive product with all M=C, M=C, and M=N intermediates, precisely the outcome found in our own experiments. Only with the coordinatively unsaturated rhodium complexes is there any evidence for competitive aryl C–H activation (a 1:3 kinetic distribution of Tp^{Me2}RhH(CNCMe₃)(CH₂C₆H₃-3,5-Me₂) and Tp^{Me2}RhH(CNCMe₃)(C₆H₂-2,4,6-Me₃)).¹⁴ Steric congestion around Nb resulting from the presence of two η^2 -coordinated ligands, 2-butyne and cyclopropene, in A appears to block aryl CH bond activation, both kinetically and thermodynamically.

For the isomers of dimethylbenzene, product distributions are rather more variable. For 1,2-dimethylbenzene, the intermediate Cp*W(NO)(=CHC₆H₅)^{5f} generates a 94:6 mixture of aryl Cp*W(NO)(CH₂C₆H₅)(3,4-Me₂C₆H₃) and benzylic Cp*W(NO)(CH₂C₆H₅)(CH₂-2-MeC₆H₄) complexes. Our niobium systems show 100% selectivity for aryl activation, suggesting that the benzylic position is slightly more accessible in the tungsten chemistry. In contrast, the 1,4-isomer reacts with the unsaturated alkylidene Cp*Mo(NO)(=CHCMe₃) (generated by α -H abstraction of neopentane from Cp*Mo(NO)(CH₂CMe₃)₂) to give a 73:27 kinetic mixture of the aryl and benzylic complexes Cp*Mo(NO)(CH₂CMe₃)(2,5-Me₂C₆H₃) and Cp*Mo(NO)(CH₂CMe₃)(η^2 -CH₂-4-MeC₆H₄).⁵ⁱ The dominance of aryl product here stands in stark contrast to the 100% benzylic selectivity displayed by 1. With 1,3-dimethylbenzene, the tungsten species Cp*W(NO)(=CHC₆H₅) generates aryl and benzylic activation products in a 90:10 ratio, not dissimilar to the 3:1 ratio observed with 1.

Thus in cases where the arene hydrogens are sterically blocked by *ortho* methyl groups on both sides (i.e., mesitylene), all reagents with unsaturated carbon- and nitrogen-based ligands give the same result: activation at the benzylic position. Similarly, in the least sterically crowded cases, where an arene hydrogen has no *ortho* methyl groups, all unsaturated intermediates give aryl C–H activation, albeit with some competitive benzylic reactivity. Only for the intermediate case of 1,4-dimethylbenzene, where all arene hydrogens lie *ortho* to one methyl group, does A show significantly different reactivity from the alkylidene intermediates reported by Legzdins and co-workers. The switch to benzylic activation with intermediate A suggests that the balance between steric and electronic factors is subtly different from that in Cp*Mo(NO)(=CHCMe₃).

Summary. Intramolecular β -H abstraction of methane from Tp^{Me2}NbMe(*c*-C₃H₅)(MeCCMe) generates an unsaturated intermediate [Tp^{Me2}Nb(η^2 -*c*-C₃H₄)(MeCCMe)] (A) that activates benzylic or aryl CH bonds of various dimethylbenzenes and mesitylene. The aromatic activation pathway is preferred, both kinetically and thermodynamically, in sterically unhindered systems. However, the presence of an *ortho* methyl group raises the barrier above that for activation of a benzylic C–H bond. As a result, benzylic activation dominates in cases where all aromatic groups lie *ortho* to a methyl group.

EXPERIMENTAL SECTION

All experiments were carried out under a dry argon atmosphere using either Schlenck tube or glovebox techniques. Benzene, pentane, mesitylene, and all dimethylbenzenes were dried by refluxing over CaH₂ under argon. Deuterated NMR solvents were dried over molecular sieves, degassed by freeze–pump–thaw cycles, and stored under argon. ¹H and ¹³C NMR spectra were obtained on Bruker ARX 250, DPX 300, or Avance 300 and 500 spectrometers. Only pertinent ¹J_{CH} are quoted in the ¹³C spectra. Tp^{Me2}NbMe(*c*-C₃H₅)(MeC≡CMe) (1) was prepared according to a published procedure.³ Elemental analyses were performed in the Analytical Service of our laboratory.

Synthesis of Tp^{Me2}Nb(CH₂-3,5-Me₂C₆H₃)(*c*-C₃H₅)(MeC≡CMe) (3). Tp^{Me2}NbMe(*c*-C₃H₅)(MeC≡CMe) (1) (0.143 g, 0.286 mmol) was gently heated in mesitylene (5 mL) at 308 K for 16 h. The color of the solution changed from yellow to dark orange. The solvent was evaporated to dryness. The residue was then extracted with pentane, and the slurry was filtered through a pad of Celite to give a dark orange solution, which was dried under vacuum. The residue was washed with 2 × 5 mL of cold pentane (–80 °C). The powder was isolated and dried

under vacuum (0.089 g, 0.147 mmol, 51%). Crystals were obtained by cooling a concentrated pentane solution of **3** at 253 K. ^1H NMR (300 MHz, benzene- d_6 , 288 K): δ 6.52 (s, 1H, 4- C_6H_3), 6.45 (s, 2H, 2- C_6H_3), 5.77, 5.65, 5.61 (all s, 1H each, $\text{Tp}^{\text{Me}_2}\text{CH}$), 2.77, 2.28 (both s, 3H each, $\text{CH}_3\text{C}\equiv$), 2.93, 2.84 (both d, $^2J_{\text{HH}} = 11.3$ Hz, 1H each, NbCH_2), 2.66, 2.29, 2.19, 2.09, 2.08, 1.71 (all s, 3H each, $\text{Tp}^{\text{Me}_2}\text{CH}_3$), 2.20 (s, 6H, $\text{C}_6\text{H}_3\text{CH}_3$), 1.94, 1.74, 1.36, 0.93 (all m, 1:1:2:1 H, $\text{CH}_2\beta$, $\text{CH}\alpha$, $\text{CH}_2\beta'$, $\text{CH}_2\beta''$). ^{13}C NMR (75.47 MHz, benzene- d_6 , 288 K): δ 240.9, 240.0 (MeC \equiv), 152.6 (Cipso), 151.7, 151.1, 150.2, 143.7, 143.6, 143.4 ($\text{Tp}^{\text{Me}_2}\text{CMe}$), 135.6 (*m*- C_6H_3), 125.3 (*o*- C_6H_3), 123.0 (*p*- C_6H_3), 107.9, 107.1, 106.9 ($\text{Tp}^{\text{Me}_2}\text{CH}$), 77.2 (br t, $^1J_{\text{CH}} = 117$ Hz, NbCH_2), 65.6 (d, $^1J_{\text{CH}} = 138$ Hz, $\text{NbC}\alpha\text{H}$), 22.3, 20.0 ($\text{CH}_3\text{C}\equiv$), 21.5 (t, $^1J_{\text{CH}} = 156$ Hz, NbCHCH_2), 11.7 (t, $^1J_{\text{CH}} = 159$ Hz, $\text{NbCHC}'\text{H}_2$), 16.3, 15.3, 14.7, 12.8, 12.7, 12.7 ($\text{Tp}^{\text{Me}_2}\text{CH}_3$). Anal. Calcd for $\text{C}_{31}\text{H}_{44}\text{BN}_6\text{Nb}$: C, 61.60; H, 7.34; N, 13.90. Found: C, 62.04; H, 7.28; N, 13.62.

Synthesis of $\text{Tp}^{\text{Me}_2}\text{Nb}(\text{CH}_2\text{-4-MeC}_6\text{H}_4)(\text{c-C}_3\text{H}_5)(\text{MeC}\equiv\text{CMe})$ (4**).** $\text{Tp}^{\text{Me}_2}\text{NbMe}(\text{c-C}_3\text{H}_5)(\text{MeC}\equiv\text{CMe})$ (**1**) (0.163 g, 0.326 mmol) was heated in 1,4-dimethylbenzene (3 mL) at 315 K for 7 h. The color of the solution changed from yellow to green. The solvent was evaporated to dryness. The residue was extracted with 5 mL of pentane and filtered through a pad of Celite. The solution was concentrated and cooled at 253 K. The resulting precipitate was washed three times with 3 mL of cold pentane (-80°C) to give an orange powder, which was dried under vacuum (0.088 g, 0.150 mmol, 46%). ^1H NMR (300 MHz, benzene- d_6 , 288 K): δ 7.01, 6.93 (d, $^2J_{\text{HH}} = 2.4$ Hz, 2 H each, $\text{NbCH}_2\text{-4-MeC}_6\text{H}_4$, 2- and 3-Hs), 5.80, 5.63, 5.62 (all s, 1H each, $\text{Tp}^{\text{Me}_2}\text{CH}$), 2.65, 2.26 (all s, 3H each, $\text{CH}_3\text{C}\equiv$), 2.92, 2.78 (d, $^2J_{\text{HH}} = 11.4$ Hz, 1H each, NbCH_2), 2.71, 2.28, 2.16, 2.09, 2.04, 1.77 (all s, 3H each, $\text{Tp}^{\text{Me}_2}\text{CH}_3$), 2.28 (s, 3H, $\text{C}_6\text{H}_4\text{CH}_3$), 1.88, 1.84, 1.36, 0.91 (all m, 1:1:2:1 H, $\text{CH}_2\beta$, $\text{NbCH}\alpha$, $\text{CH}_2\beta'$, $\text{CH}_2\beta''$). $^{13}\text{C}\{^1\text{H}\}$ NMR (75.47 MHz, benzene- d_6 , 288 K): δ 241.9, 241.2 (MeC \equiv), 150.6 (Cipso), 151.8, 151.1, 150.4, 144.0, 143.8, 143.5 ($\text{Tp}^{\text{Me}_2}\text{CMe}$), 130.0 (4- C_6H_4), 128.1, 127.0 (*m*, *o*- C_6H_4), 108.2, 107.3, 107.0 ($\text{Tp}^{\text{Me}_2}\text{CH}$), 76.5 (br t, $^1J_{\text{CH}} = 117$ Hz, NbCH_2Ar), 67.2 (d, $^1J_{\text{CH}} = 138$ Hz, $\text{NbC}\alpha\text{H}$), 22.4 ($\text{C}_6\text{H}_4\text{CH}_3$), 21.0, 20.2 ($\text{CH}_3\text{C}\equiv$), 21.7, 12.5 (t, $^1J_{\text{CH}} = 158$, 160 Hz, $\text{C}\beta'$, $\text{C}\beta$), 16.5, 15.4, 15.2, 13.0, 12.9, 12.8 ($\text{Tp}^{\text{Me}_2}\text{CH}_3$). Anal. Calcd for $\text{C}_{30}\text{H}_{42}\text{BN}_6\text{Nb}$: C, 61.03; H, 7.17; N, 14.23. Found: C, 61.55; H, 7.52; N, 13.92.

Synthesis of $\text{Tp}^{\text{Me}_2}\text{Nb}(\text{3,4-Me}_2\text{C}_6\text{H}_3)(\text{c-C}_3\text{H}_5)(\text{MeC}\equiv\text{CMe})$ (5**).** $\text{Tp}^{\text{Me}_2}\text{NbMe}(\text{c-C}_3\text{H}_5)(\text{MeC}\equiv\text{CMe})$ (**1**) (0.138 g, 0.28 mmol) was stirred in 1,2-dimethylbenzene (3 mL) at ambient temperature for 20 h. The color of the solution changed from yellow to orange. The solvent was evaporated to dryness. The residue was extracted with 5 mL of pentane and filtered through a pad of Celite. An orange powder containing an inseparable mixture of **5** and the diaryl derivative (9:1 ratio) was obtained after drying under vacuum (0.168 g, 0.28 mmol, 100%). ^1H NMR (300 MHz, benzene- d_6 , 288 K): δ 6.81 (br s, 3H, $\text{NbC}_6\text{H}_3\text{Me}_2$), 5.75, 5.74, 5.62 (all s, 1H each, $\text{Tp}^{\text{Me}_2}\text{CH}$), 3.06, 2.28 (all s, 3H each, $\text{CH}_3\text{C}\equiv$), 2.28, 2.20, 2.18, 2.16, 1.90, 1.40 (all s, 3H each, $\text{Tp}^{\text{Me}_2}\text{C}_6\text{H}_3$), 2.06, 2.05 (s, 3H each, $\text{C}_6\text{H}_3\text{CH}_3$), 2.27, 2.06, 1.65, 1.42, 0.93 (all m, 1H each, $\text{CH}_2\beta$, $\text{NbCH}\alpha$, $\text{CH}_2\beta'$, $\text{CH}_2\beta''$, $\text{CH}_2\beta$). ^1H NMR (500 MHz, dichloromethane- d_2 , 193 K) only dynamic aromatic protons are quoted: δ 8.16 (s, 1H, $\text{NbC}_6\text{H}_3\text{Me}_2$ 2-H), 6.43, 5.71 (d, $^2J_{\text{HH}} = 13.8$ Hz, 1H each, $\text{NbC}_6\text{H}_3\text{Me}_2$ 5- and 6-H). $^{13}\text{C}\{^1\text{H}\}$ NMR (75.47 MHz, benzene- d_6 , 288 K): δ 241.6, 239.5 (MeC \equiv), 190.9 ($\text{NbC}_6\text{H}_3\text{Me}_2$), 153.2, 151.1, 151.0, 143.8, 143.5, 143.3 ($\text{Tp}^{\text{Me}_2}\text{CCH}_3$), 138.9, 135.4, 134.0, 133.2, 132.6 ($\text{C}_6\text{H}_3\text{Me}_2$), 107.6, 107.1, 107.1 ($\text{Tp}^{\text{Me}_2}\text{CH}$), 70.7 (br, $\text{NbC}\alpha\text{H}$), 20.0, 19.8 ($\text{C}_6\text{H}_3(\text{CH}_3)_2$), 22.5, 19.4 ($\text{CH}_3\text{C}\equiv$), 21.9, 12.9 ($\text{C}\beta'$, $\text{C}\beta$), 15.5, 15.5, 14.9, 13.0, 12.8, 12.8 ($\text{Tp}^{\text{Me}_2}\text{CH}_3$).

Reaction of **1 with 1,3-Dimethylbenzene to Give a Mixture of $\text{Tp}^{\text{Me}_2}\text{Nb}(\text{c-C}_3\text{H}_5)(\text{3,5-Me}_2\text{C}_6\text{H}_3)(\text{MeC}\equiv\text{CMe})$ (**6-Ar**) and $\text{Tp}^{\text{Me}_2}\text{Nb}(\text{3-MeC}_6\text{H}_4)(\text{c-C}_3\text{H}_5)(\text{MeC}\equiv\text{CMe})$ (**6-Bz**).** $\text{Tp}^{\text{Me}_2}\text{NbMe}(\text{c-C}_3\text{H}_5)(\text{MeC}\equiv\text{CMe})$ (**1**) (0.200 g, 0.40 mmol) was stirred in 1,3-dimethylbenzene (4 mL) at 35°C for 6 h. The color of the solution changed from yellow to orange. The solvent was evaporated to dryness.

The residue was extracted with 15 mL of pentane and filtered through a pad of Celite. An orange powder was obtained, which contained (^1H NMR) **1** (32%), **6-Ar** (34%), and **6-Bz** (12%) together with 22% of ill-defined complexes. Separated kinetic experiments have been carried out, and the ratio **6-Ar**:**6-Bz** \approx 3:1 remained constant throughout the course of the reaction. Out of the complex mixture, **6-Ar** and **6-Bz** were unambiguously and repeatedly identified, although several NMR signals are missing/obscured and could not be assigned with confidence. For **6-Ar**. ^1H NMR (300 MHz, cyclohexane- d_{12} , 288 K): δ 6.53 (s, $\text{NbC}_6\text{H}_3\text{Me}_2$, 3-H), 5.71, 5.66, 5.58 (all s, 1H each, $\text{Tp}^{\text{Me}_2}\text{CH}$), 3.02, 2.22 (all s, 3H each, $\text{CH}_3\text{C}\equiv$), 2.47, 2.40, 2.38, 2.10, 1.64, 1.19 (all s, 3H each, $\text{Tp}^{\text{Me}_2}\text{CH}_3$), 1.95, 1.81, 1.46, 1.24, 0.75 (all m, 1H each, $\text{CH}_2\beta$, $\text{NbCH}\alpha$, $\text{CH}_2\beta'$, $\text{CH}_2\beta''$, $\text{CH}_2\beta$). $^{13}\text{C}\{^1\text{H}\}$ NMR (75.47 MHz, cyclohexane- d_{12} , 288 K): δ 241.4, 239.0 (MeC \equiv), 193.0 ($\text{NbC}_6\text{H}_3\text{Me}_2$), 141–154 ($\text{Tp}^{\text{Me}_2}\text{CCH}_3$), 127–135 ($\text{C}_6\text{H}_3\text{Me}_2$), 107.3, 107.1, 106.7 ($\text{Tp}^{\text{Me}_2}\text{CH}$), 70.5 (br, $\text{NbC}\alpha$), 21.5, 19.1 ($\text{CH}_3\text{C}\equiv$), 15.4, 15.1, 14.7, 13.1, 13.0, 13.0 ($\text{Tp}^{\text{Me}_2}\text{CH}_3$). For **6-Bz**. ^1H NMR (300 MHz, cyclohexane- d_{12} , 288 K): δ 6.80 (pt, 1H, $^3J_{\text{HH}} = 7.5$ Hz, $\text{C}_6\text{H}_4\text{Me}$, 4-H), 6.48, 6.46 (d, 1H each, $^3J_{\text{HH}} = 7.5$ Hz, $\text{C}_6\text{H}_4\text{Me}$, 3- and 5-H), 6.21 (s, 1H, $\text{C}_6\text{H}_4\text{Me}$, 2-H), 5.79, 5.65, 5.62 (all s, 1H each, $\text{Tp}^{\text{Me}_2}\text{CH}$), 3.14, 2.35 (all s, 3H each, $\text{CH}_3\text{C}\equiv$), 2.64, 2.45 (d, $^2J_{\text{HH}} = 8.9$ Hz, 1H each, $\text{NbCH}_2\text{C}_6\text{H}_4\text{Me}$), 2.61, 2.45, 2.38, 2.33, 1.99, 1.65 (all s, 3H each, $\text{Tp}^{\text{Me}_2}\text{CH}_3$), 2.09 (s, 6H, $\text{C}_6\text{H}_4\text{CH}_3$). $^{13}\text{C}\{^1\text{H}\}$ NMR (75.47 MHz, cyclohexane- d_{12} , 288 K): δ 127.9 ($\text{C}_6\text{H}_4\text{Me}_2$, 2-C, 127.0 ($\text{C}_6\text{H}_4\text{Me}_2$, 4-C, 124.5, 122.0 ($\text{C}_6\text{H}_4\text{Me}_2$, 5- and 6-C), 77.1 ($\text{NbCH}_2\text{C}_6\text{H}_4\text{Me}_2$), 66.3 ($\text{NbC}\alpha$).

Kinetics of the Reaction between **1 and Mesitylene, 1,4-Dimethylbenzene, or 1,4-Dimethylbenzene- d_{10} .** The same procedure was used for the three cases; that with mesitylene is described herein. Under argon, a weighed amount of **1** (ca. 10^{-4} mmol) was introduced in a screw-cap NMR tube. Cyclohexane- d_{12} was added so that the total volume (cyclohexane- d_{12} + arene) was 0.5 mL. The appropriate amount of mesitylene (see text) was added dropwise with a microsyringe. The tube was then placed in the preheated ($T = 308$ K) NMR probe of the AV300 spectrometer. Acquisitions of ^1H NMR spectra started 10 min later to allow temperature equilibration. Each acquisition was composed of eight scans with a 13 s delay between scans (total acquisition time 2 min).

X-ray Crystallography. Data for **3** were collected at 180 K on a Bruker Kappa Apex II diffractometer using graphite-monochromated Mo K α radiation ($\lambda = 0.71073$ Å) and equipped with an Oxford Instrument cooler device. The final unit cell parameters have been obtained by means of a least-squares refinement on a set of 7452 well-measured reflections. Orange crystal, $\text{C}_{31}\text{H}_{44}\text{BN}_6\text{Nb}$; fw 604.4 g·mol $^{-1}$, triclinic, $P\bar{1}$, $a = 10.3669(5)$ Å, $b = 11.0238(5)$ Å, $c = 14.7350(7)$ Å, $\alpha = 93.515(2)^\circ$, $\beta = 95.803(2)^\circ$, $\gamma = 114.082(2)^\circ$, $V = 11519.72(12)$ Å 3 , $T = 180(2)$ K, $Z = 2$, final R indices [$I > 2\sigma(I)$]: $R1 = 0.0427$, $wR2 = 0.1114$, goodness-of-fit on F^2 : 1.301.

The structure has been solved by direct methods using SHELXS-86 16 and refined by means of least-squares procedures on F^2 with the aid of the program SHELXL97 16 included in the software package WinGX version 1.63. 17 The atomic scattering factors were taken from the International Tables for X-ray Crystallography. 18 All hydrogen atoms were geometrically placed and refined by using a riding model. All non-hydrogen atoms were anisotropically refined, and in the last cycles of refinement a weighting scheme was used, where weights were calculated from the following formula: $w = 1/[\sigma^2(F_o^2) + (aP)^2 + bP]$ where $P = (F_o^2 + 2F_c^2)/3$. Plot of the molecular structure was performed with the program ORTEP3 19 with 30% probability displacement ellipsoids for non-hydrogen atoms.

Computational Details. Calculations were performed by DFT methods with the PBE1PBE functional, 20 as implemented in Gaussian03. 21 Nb was described using the LANL2DZ effective core potential for the inner electrons and its associated basis set for the outer ones. 22 An f polarization shell was added (exponent 0.952). 23 The standard 6-31G(d) 24

basis set was used for all other atoms. Stationary points and transition states were fully optimized without any symmetry restriction. Transition states were identified by having one imaginary frequency. All reported values correspond to potential energies with zero-point energy corrections unless otherwise stated. In the case of aromatic activation of 1,4-dimethylbenzene, we performed an additional set of calculations with the ONIOM(PBE1PBE:UFF) method,^{25,26} where the *ortho* methyl substituent was placed in the MM region.

■ ASSOCIATED CONTENT

S Supporting Information. Full ref 21, computed reaction profiles with potential and Gibbs free energy values for all methylbenzene compounds, absolute energies and Cartesian coordinates for all computed structures, key NMR spectra for the reactions giving **5** and **6-Bz** and **6-Ar**, and a CIF file for the X-ray structure of **3**. This material is available free of charge via the Internet at <http://pubs.acs.org>.

■ AUTHOR INFORMATION

Corresponding Author

*E-mail: michel.etienne@lcc-toulouse.fr.

■ ACKNOWLEDGMENT

M.E. thanks the ANR program (BLAN07-2_182861) and the CNRS (LEA 368, LTPMM) for funding and the Université Paul Sabatier for a sabbatical leave. M.E. and J.E.M. thank the Royal Society for a Short Visit incoming Grant and the Royal Society of Chemistry for a Grant to International Authors. A.L. and F.M. thank the Spanish MICINN (projects CTQ2008-06866-CO2-02/BQU and Consolider Ingenio 2010 CSD2006-0003) and the ICIQ Foundation for financial support.

■ REFERENCES

- (1) (a) See Special Issue of *Chemical Reviews* on "Selective Functionalization of C-H Bonds": Crabtree, R. H. *Chem. Rev.* **2010**, *110*, 575. (b) Jazsar, R.; Hitce, J.; Renaudat, A.; Sofack-Freutzer, J.; Baudoin, O. *Chem.—Eur. J.* **2010**, *16*, 2654. (c) Bergman, R. G. *Nature* **2007**, *446*, 391. (d) Goldberg, K. I.; Goldman, A. S., Eds. *Activation and Functionalization of C-H Bonds*; ACS Symposium Series 885; American Chemical Society: Washington, DC, 2004.
- (2) (a) Balcells, D.; Clot, E.; Eisenstein, O. *Chem. Rev.* **2010**, *110*, 749. (b) Vastine, B. A.; Hall, M. B. *Coord. Chem. Rev.* **2009**, *253*, 1202. (c) Perutz, R. N.; Sabo-Etienne, S. *Angew. Chem., Int. Ed.* **2007**, *46*, 2578. (d) Jones, W. D. *Inorg. Chem.* **2005**, *44*, 4475. (e) Lersch, M.; Tilset, M. *Chem. Rev.* **2005**, *105*, 2471. (f) Labinger, J. A.; Bercaw, J. E. *Nature* **2002**, *417*, 507.
- (3) (a) Boulho, C.; Oulié, P.; Vendier, L.; Etienne, M.; Pimienta, V.; Locati, A.; Bessac, F.; Maseras, F.; Pantazis, D. A.; McGrady, J. E. *J. Am. Chem. Soc.* **2010**, *132*, 14239. (b) Oulié, P.; Boulho, C.; Vendier, L.; Coppel, Y.; Etienne, M. *J. Am. Chem. Soc.* **2006**, *128*, 15962.
- (4) Thompson, M. E.; Baxter, S. M.; Bulls, A. R.; Burger, B. J.; Nolan, M. C.; Santarsiero, B. D.; Schaefer, W. P.; Bercaw, J. E. *J. Am. Chem. Soc.* **1987**, *109*, 203.
- (5) (a) van der Heiden, H.; Hessen, B. *J. Chem. Soc., Chem. Commun.* **1995**, 145. (b) Coles, M. P.; Gibson, V. C.; Clegg, W.; Elsegood, M. R.; Porelli, P. A. *J. Chem. Soc., Chem. Commun.* **1996**, 1963. (c) Tran, E.; Legzdins, P. *J. Am. Chem. Soc.* **1997**, *119*, 5071. (d) Cheon, J.; Rogers, D. M.; Girolami, G. S. *J. Am. Chem. Soc.* **1997**, *119*, 6804. (e) Adams, C. S.; Legzdins, P.; Tran, E. *J. Am. Chem. Soc.* **2001**, *123*, 612. (f) Adams, C. S.; Legzdins, P.; Tran, E. *Organometallics* **2002**, *21*, 1474. (g) Wada, K.; Pamplin, C. B.; Legzdins, P. *J. Am. Chem. Soc.* **2002**, *124*, 9680. (h) Adams, C. S.; Legzdins, P.; McNeil, W. S. *Organometallics* **2001**, *20*, 4939. (i) Wada, K.; Pamplin, C. B.; Legzdins, P.; Patrick, B. O.; Tsyba, I.; Bau, R. *J. Am. Chem. Soc.* **2003**, *125*, 7035. (j) Andino, J. G.; Kilgore, U. J.; Pink, M.; Ozarowski, A.; Krzystek, J.; Telsler, J.; Baik, M.-H.; Mendiola, D. *Chem. Sci.* **2010**, *1*, 351. (k) Zhang, S.; Tamm, M.; Nomura, K. *Organometallics* **2011**, *30*, 2712.
- (6) (a) Bailey, B. C.; Fan, H.; Baum, E. W.; Huffman, J. C.; Baik, M.-H.; Mendiola, D. *J. Am. Chem. Soc.* **2005**, *127*, 16016. (b) Bailey, B. C.; Fan, H.; Huffman, J. C.; Baik, M.-H.; Mendiola, D. *J. Am. Chem. Soc.* **2006**, *128*, 6798. (c) Bailey, B. C.; Huffman, J. C.; Mendiola, D. *J. Am. Chem. Soc.* **2007**, *129*, 5302. (d) Bailey, B. C.; Fan, H. J.; Huffman, J. C.; Baik, M.-H.; Mendiola, D. *J. Am. Chem. Soc.* **2007**, *129*, 8781.
- (7) Buchwald, S. L.; Kreutzer, K. A.; Fisher, R. A. *J. Am. Chem. Soc.* **1990**, *112*, 4600.
- (8) (a) Erker, G. *J. Organomet. Chem.* **1977**, *134*, 189. (b) Fagan, P. J.; Manriquez, J. M.; Maatta, E. A.; Seyam, A. M.; Marks, T. J. *J. Am. Chem. Soc.* **1981**, *103*, 6650. (c) Wada, K.; Pamplin, C. B.; Legzdins, P. *J. Am. Chem. Soc.* **2002**, *124*, 9680. (d) Pamplin, C. B.; Legzdins, P. *Acc. Chem. Res.* **2003**, *36*, 223.
- (9) (a) Ng, S. H. K.; Adams, C. S.; Hayton, T. W.; Legzdins, P.; Patrick, B. O. *J. Am. Chem. Soc.* **2003**, *125*, 15210. (b) Tsang, J. Y. K.; Buschhaus, M. S. A.; Graham, P. M.; Semiao, C. J.; Semproni, S. P.; Kim, S. J.; Legzdins, P. *J. Am. Chem. Soc.* **2008**, *130*, 3652. (c) Debad, J. D.; Legzdins, P.; Lumb, S. A.; Batchelor, R. J.; Einstein, F. W. B. *J. Am. Chem. Soc.* **1995**, *117*, 3288. (d) Debad, J. D.; Legzdins, P.; Lumb, S. A.; Rettig, S. J.; Batchelor, R. J.; Einstein, F. W. B. *Organometallics* **1999**, *18*, 3414.
- (10) (a) Jaffart, J.; Cole, M. L.; Etienne, M.; Reinhold, M.; McGrady, J. E.; Maseras, F. *Dalton Trans.* **2003**, 4057. (b) Jaffart, J.; Etienne, M.; Reinhold, M.; McGrady, J. E.; Maseras, F. *Chem. Commun.* **2003**, 876.
- (11) Boulho, C.; Keys, T.; Coppel, Y.; Vendier, L.; Etienne, M.; Locati, A.; Bessac, F.; Maseras, F.; Pantazis, D. A.; McGrady, J. E. *Organometallics* **2009**, *28*, 940.
- (12) As with virtually all the other aryl complexes in this study, **5** subsequently reacts more slowly with a second equivalent of the arene, yielding diaryl complexes; see ref 3. Depending on the relative rates of the two reactions, it sometimes proved impossible to stop the reaction at the first stage or eventually to separate the complexes from the resulting mixtures, so that elementary analyses could be not obtained in this case.
- (13) (a) de With, J.; Horton, A. D. *Angew. Chem., Int. Ed. Engl.* **1993**, *32*, 903. (b) Hoyt, H. M.; Bergman, R. G. *Angew. Chem., Int. Ed.* **2007**, *46*, 5580. (c) Bennet, J. L.; Wolczanski, P. T. *J. Am. Chem. Soc.* **1997**, *119*, 10696. (d) Schaller, C. P.; Cummins, C. C.; Wolczanski, P. T. *J. Am. Chem. Soc.* **1996**, *118*, 591.
- (14) Jones, W. D.; Hessel, E. T. *J. Am. Chem. Soc.* **1993**, *115*, 554.
- (15) (a) Jones, W. D.; Feher, F. J. *Acc. Chem. Res.* **1989**, *22*, 91. (b) Jones, W. D. *Acc. Chem. Res.* **2003**, *36*, 140.
- (16) Sheldrick, G. M. *Acta Crystallogr. A* **2008**, *A64*, 112.
- (17) Farrugia, L. J. *Appl. Crystallogr.* **1999**, *32*, 837.
- (18) *International Tables for X-Ray Crystallography*; Kynoch Press: Birmingham, England, 1974; Vol IV.
- (19) Farrugia, L. J. *Appl. Crystallogr.* **1997**, *30*, 565.
- (20) Perdew, J. P.; Burke, K.; Ernzerhof, M. *Phys. Rev. Lett.* **1996**, *77*, 3865.
- (21) Frisch, M. J.; et al. *Gaussian 03*, Revision C.02; Gaussian, Inc.: Wallingford, CT, 2004.
- (22) (a) Hay, P. J.; Wadt, W. R. *J. Chem. Phys.* **1985**, *82*, 299. (b) Wadt, W. R.; Hay, P. J. *J. Chem. Phys.* **1985**, *82*, 284.
- (23) Ehlers, A. W.; Bohme, M.; Dapprich, S.; Gobbi, A.; Hollwarth, A.; Jonas, V.; Kohler, K. F.; Stegmann, R.; Veldkamp, A.; Frenking, G. *Chem. Phys. Lett.* **1993**, *208*, 111.
- (24) (a) Francl, M. M.; Pietro, W. J.; Hehre, W. J.; Binkley, J. S.; Gordon, M. S.; Defrees, D. J.; Pople, J. A. *J. Chem. Phys.* **1982**, *77*, 3654. (b) Hehre, W. J.; Ditchfie, R.; Pople, J. A. *J. Chem. Phys.* **1972**, *56*, 2257.
- (25) (a) Maseras, F.; Morokuma, K. *J. Comput. Chem.* **1995**, *16*, 1170. (b) Vreven, T.; Morokuma, K. *J. Comput. Chem.* **2000**, *21*, 1419.
- (26) Rappe, A. K.; Casewit, C. J.; Colwell, D. S.; Goddard, W. A.; Skiff, W. N. *J. Am. Chem. Soc.* **1992**, *114*, 10024.